2018-08-23

Automated mapping of relict patterned ground: An approach to evaluate morphologically subdued landforms using unmanned-aerialvehicle and structure-from-motion technologies

Mather, Anne

10.1177/0309133318788966
Progress in Physical Geography
SAGE Publications

Automated mapping of relict patterned ground: an approach to evaluate morphologically subdued landforms using Unmanned-Aerial-Vehicles and Structure-from-Motion technologies

[1]Mather AE, [1]Fyfe RM, [1]Clason CC, [1]Stokes, M, [1]Mills, S and [2]Barrows, T. T.

[1]School of Geography, Earth and Environmental Sciences, University of Plymouth, Plymouth, PL4 8AA

[2]Department of Geography, Universities of Portsmouth and Wollongong, Exeter EX4 4RJ

Acknowledgements

The authors would like to thank the assistance of Joes Hess (Maristow Estate) and Robert Andrew (Southwest Water) for permission to fly at Leeden Tor, together with Graham Cotton (Peakhill Farm), Robert Steemson (Dartmoor National Park Authority Head Ranger), Tim Absalom (Plymouth University Cartography Unit) and Maisie Mather for support in coordinating the successful flight missions.

Automated mapping of relict patterned ground: an approach to evaluate morphologically subdued landforms using Unmanned-Aerial-Vehicles and Structure-from-Motion technologies

Abstract

Relict landforms provide a wealth of information on the evolution of the modern landscape and climate change in the past. To improve understanding of the origin and development of these landforms we need better spatial measurements across a variety of scales. This can be challenging using conventional surveying techniques due to difficulties in landform recognition on the ground (e.g. weak visual/topographic expression) and spatially variable areas of interest. Here we explore the appropriateness of existing remote sensing data sets (aerial LiDAR and aerial photography) and newly acquired Unmanned Aerial Vehicle (UAV) imagery of a test site on the upland of Dartmoor in SW England (Leeden Tor) for the recognition and automated mapping of relict patterned ground composed of stripes and polygons. We find that the recognition of these landforms is greatly enhanced by automated mapping using spectral 2D imagery. Image resolution is important, with the recognition of elements (boulders) of <1m maximised from the highest resolution imagery (Red-Green-Blue UAV) and recognition of landforms (10-100 m scale) maximised on coarser resolution aerial imagery. Topographic metrics of these low relief (0.5 m) landforms is best extracted from structure-from-motion (SfM) processed UAV true-colour imagery, and in this context the airborne LiDAR data proved less effective. Integrating automated mapping using spectral attributes and SfM-derived Digital Surface Models (DSMs) from UAV RGB imagery provides a powerful tool for rapid reconnaissance of field sites to facilitate the extraction of meaningful topographic and spatial metrics that can inform on the origin of relict landform features. Care should be given to match the scale of features under consideration to the appropriate scale of datasets available.

Keywords

Periglacial, structure-from-motion, Dartmoor, UAV, spatial scale, patterned ground, automated mapping

Introduction

The advent of Unmanned Aerial Vehicles (UAV) has proved to be a major advance in airborne remote sensing, offering both a cost-effective and temporally-flexible method of image acquisition that can complement or indeed substitute the traditional remote sensing platforms of manned aircraft and satellites. In addition to provision of high resolution 2D imagery, the use of a UAV provides an alternative method for development of Digital Elevation Models (DEMs), which here we take to include both Digital Surface Models (DSMs of the earth surface and all objects upon it, thus including vegetation) and Digital Terrain Models (DTMs of the bare earth surface, not including vegetation). This is achieved via structure-from-motion (SfM) and now more than rivals manned airborne and spaceborne LiDAR (Light Detection and Ranging), interferometry, photogrammetry, and radar altimetry, in addition to ground-based surveys, in terms of cost, portability, and rapidity of data collection (e.g. Westoby et al 2012; Fonstad et al 2013; Piermattei et al, 2016). SfM is a form of photogrammetry which utilises algorithms to identify matching points between overlapping images to produce a 3D surface (Carrivick et al., 2016), and can be conducted within a range of computer software packages and web- or smartphone-based apps (Micheletti et al., 2015a). Given the relatively close range of typical UAV-based data collection (usually <100m above the ground surface), the images acquired are very high resolution (typically <10 cm), even when using consumer-grade digital cameras. By using suitable ground control points or a real-time kinematic global navigation satellite system (RTK GNSS) capability to constrain elevation, SfM-derived DSMs are more accurate and precise than DEMs produced using airborne LiDAR (e.g. Carrivick et al 2016). The SfM workflow is thus a tool increasingly used within the geoscience community as UAV and data processing technology becomes more affordable and accessible (Westoby et al., 2012; Micheletti et al., 2015b; Smith et al., 2016), bridging the gap between spatially extensive but often expensive traditional remote image acquisition and high resolution but spatially-restricted and labour-intensive, ground-based data collection.

SfM has been used for a broad range of geoscience applications, including landslide monitoring (e.g. Lucieer et al., 2013), reconstruction of flood magnitude (e.g. Smith et al., 2014), mapping of coastal environments (e.g. Mancini et al., 2013), and topographic surveying (e.g. Tonkin et al., 2014). The relatively low cost of UAV image acquisition also means that SfM is not only useful for 'one time only' mapping, but also in understanding Earth surface processes, where access for repeat survey is possible. While SfM is being employed more frequently for the study of cryospheric processes and glacial landforms (e.g. Immerzeel et al., 2014; Nolan et al., 2015; Ryan et al., 2015; Westoby et al., 2015; Ely et al., 2016; Evans et al 2016), its use in the study of periglacial activity and landforms has been

very limited to date, with a small number of studies on rock glaciers and high-Arctic alluvial fans (e.g. Gómez-Gutiérrez et al., 2014; Haas et al 2015; Piermattei et al., 2016) and fewer still specifically on periglacial patterned ground (e.g. Kääb et al., 2014). In their study of patterned ground in Spitsbergen, Kääb et al. (2014) employed repeat ground-based photography alongside SfM and feature tracking to better understand the evolution of sorted circles, reporting vertical precision on the order of ±6 mm. This level of accuracy, combined with opportunity for repeat image acquisition, champions the use of SfM not only for geomorphological mapping, but also for process geomorphology, even at the micro-topographic scale.

It is thus evident that the repeated and high resolution (<5 m) DSMs that can be generated from UAV survey imagery have significant potential for informing the study of process and environmental change in glacial and periglacial environments (e.g. Abermann et al 2010; Kääb et al., 2014). In more recent years both ground and airborne LiDAR have fulfilled this data niche. The use of SfM to build DSMs from UAV-derived data has potential to contribute in these areas and to bridge some of the spatial resolution gaps currently experienced from commercially available LiDAR. In investigations of DEM accuracy (eg Boulton and Stokes 2018) and comparability with ground based traditional survey (using a total station), UAV imagery processed through SfM software has compared favourably (e.g. Kršák et al 2016). Piermattei et al. (2016) compared airborne LiDAR against handheld ground-based digital RGB imagery, processed through SfM software to produce a DSM of a rock glacier. These researchers found that processing times on the non-georeferenced images were long (10 days, though this is clearly dependent on individual hardware and software capabilities), but that the level of expertise required for processing was lower than that required for LiDAR and traditional photogrammetry. They estimated the SfM DSM accuracy of the reconstructed rock glacier surface to be 0.02 m - 0.17 m. Using a UAV (GPS enabled) both improves the spatial coverage and thus accuracy of the potential SfM DSM, speeds up data acquisition (for the surveys presented in this paper, an aircraft mission that can survey 300 x 300m typically takes less than 15 mins for a double grid criss-cross flight mission to optimize SfM DSM generation) and reduces the problems of processing time.

The particular geomorphological challenges in collecting reliable metrics to analyse active and relict patterned ground in periglacial environments are common to the understanding of other landforms that may be problematic to recognise at ground level using traditional techniques. For example, the topographic data need to be high enough resolution to discern subtle relief features and also allow time-efficient mapping of the distribution of features that are visually challenging to determine at ground level over wide areas. To evaluate the efficacy of SfM and UAV imagery in delineating and analysing such features, we focus here

on the collection of a range of remotely-sensed data sets, and evaluate their effectiveness for describing and identifying relict sorted and patterned ground which may have a linear or polygonal structure. This will be achieved by integrating both optical imagery (spectral signature) and topographic metrics to enable automated mapping on a field site near Leeden Tor, Dartmoor in the UK (Fig. 1). Recommendations based on this experience will be presented for wider application of these approaches. Further additional work will build on these observations to examine the process origins of the features considered.

[insert Figure 1]

Study area

Dartmoor has long been upheld as an archetypal example of a relict periglacial environment characterised by suites of mature periglacial landforms. Those identified include gelifluction deposits, altiplanation terraces, block-fields and patterned ground (Te Punga, 1956; Palmer and Nielsen 1962; Waters, 1964; Gerrard, 1988; Bennett et al., 1996; Evans et al., 2012a). Recent research by Evans et al. (2012a; 2012b) alludes to the possibility that Dartmoor may also have been subject to glaciation during the Pleistocene, contrasting with previously held views of the extent of Pleistocene glaciation in the UK (e.g. Chiverrell & Thomas, 2010). The icefield-style glaciation of north and central Dartmoor theorised by Evans et al. (2012a) has been offered as an explanation to why some perceived periglacial landforms in north Dartmoor are alleged to be less developed in comparison to those found in surrounding areas (Evans et al., 2017), although more rigorous regional mapping is required to verify this. It is surprising, therefore, that despite the established and emerging research regarding the nature and distribution of periglaciation in the uplands of SW England, systematic mapping of the features found across extensive areas of Dartmoor has hitherto not been undertaken (Evans et al 2017). This, in part, reflects Dartmoor's large size (954 km^2), and that as a protected landscape with only rare subsurface sections through often both relict *and* polygenetic landform features, landscape interpretation can be challenging. Emerging technologies provide the opportunity to undertake more rigorous terrain evaluation of extensive areas and have stimulated a revisit of the origins of the 'classic' relict periglacial landforms that occur over wide areas of Dartmoor.

The study area, Leeden Tor is a castellated tor standing at 389 m a.s.l. and situated in the south-west of Dartmoor National Park (Fig. 1) and approximately 3.5 km south-west of the village of Princetown. The area around the tor is developed on microgranite with loam soil cover in places, and the surrounding slopes by more typical Dartmoor granite covered with sandy loam. The tor has an apparent ^{10}Be exposure age of ~100 ka (Gunnell et al 2013). The study site discussed here is located on a tor-free summit, immediately south of Leeden

Tor, at an elevation of 385 m a.s.l. and covering 0.42km^2 (Fig. 1). This site has been chosen due to its accessibility, limited vegetation cover and the presence of sorted patterned ground ranging from stripes to polygons (Fig. 2).

[insert Figure 2]

In addition to patterned ground, the south-facing slopes of Leeden Tor also play host to a number of stone hut circles (Fig. 1) that are evidence of Bronze Age settlement at this site (Fleming 2008). While these hut circles are obvious as positive reliefs (~0.5-1m) both on the ground (Fig. 2C) and from the air at Leeden Tor (Fig. 3), it is worth exercising caution when interpreting upland landscapes in south-west England, particularly with regard to human reworking of clitter (boulder fields) either as part of a process of appropriation or augmentation of natural features (Bradley 2000; Tilley et al., 2000). On a more prosaic level, readily-available stone is likely to have been exploited during the construction of the abundant prehistoric hut circles and field walls across the southwest uplands. Additionally, the lower slopes of Leeden Tor have been manually quarried and large boulders removed, most probably for the construction of the Princetown toll road in 1812 (Ebdon 2014). The artificially sharp breaks of slope show up clearly in DEMs of the site (Fig. 3F).

[insert Figure 3]

Approach, methods and datasets

In this paper we develop and evaluate methodologies for automated mapping of relict, sorted patterned ground. It is beyond the scope of this paper to examine detailed process origins for the features. Rather we wish to focus on the process of extracting useful information on form and location (the nature of being or 'ontology' of the patterned ground) that will inform on-going future analyses of landform origin as part of a more extensive and rigorous assessment of the Dartmoor area that has hitherto not been possible by traditional technologies.

Object ontologies for the sorted, patterned ground

In the field: Identifying relict patterned ground is often challenging at very close proximity in the field due to the subtle topographic expression and physical size of some features (Fig. 2). In areas such as Dartmoor this recognition is made even more challenging from the ground by the low slope angles and lack of vantage points for distant viewing and low vegetation cover hindering clarity of expression of the features. In this paper we utilise generic, descriptive terms for the features observed, rather than inferring process of origin. Boulder fields across Dartmoor tend to be arranged into sorted and patterned ground that takes the form of stripes, runs and garlands (e.g. Gerrard 1988). Here we use the term

'sorted patterned ground' in a non-genetic sense to describe largely linear to polygonal clustering of boulders, typically in a subtle negative relief where the bare stones that comprise the landforms occur in topographic lows of <0.5 m (e.g. Figs 2 A,B,D). Where the patterned ground forms more polygonal structures (Fig 2) they are clearly distinguishable from hut circles by their more modest negative relief and smaller size (contrast Figs 2C and 2D). For simplicity we refer to the specific geomorphometry of the patterned ground as landforms as they have a recognisable shape (MacMillan and Shary 2009; Evans 2012). Unlike drumlins or cirques these landforms cannot be clearly defined as distinct objects, and are composed of what we refer to here as 'elements' (a sub-component of the landform), which in this case are individual sub-meter scale boulders (Fig. 2).

Remotely: Identification of geomorphic features within a programme of field mapping involves a combination of agreed definitions (as outlined above), normally based on morphometric properties and expert knowledge suitable for the recognition of these properties, to develop a geomorphological signature (Giles 1998). Moving from field- to remote sensing-based mapping essentially involves a similar process: expert knowledge is used to classify features identified within imagery into a series of established geomorphic features (e.g. Smith et al 2006). In the case of the relict periglacial geomorphology of Dartmoor, features are evident on vertical aerial imagery as polygonal and linear arrangements of boulders, with the exact form of these periglacial features controlled by local topography (Fig 2). Manual digitising of geomorphic features is possible, but has long been considered within the GIS literature as potentially error-prone (Goodchild 1987), largely as a result of positional error in the manual digitisation process (e.g. Santangelo et al 2015). Similar landforms have been manually mapped at Great Mis Tor (Green and Eden, 1973; Harrison et al. 1996) using traditional techniques. Automated feature extraction is now possible within geomorphology at the landform level (Drăguţ and Blaschke, 2006), drawing upon spectral and topographic (e.g. slope gradient and convexity) characteristics for particular types of landform (e.g. Martha et al., 2010; Telfer et al., 2015). We explore the extent to which mapping sorted patterned ground can be automated across datasets of different spatial resolution.

In order to automatically extract the patterned ground, object-based ontologies are required, that is, the landform features must be identified according to objective rules. For the purposes of this study, the formal ontology of patterned ground (the landform) is a group of boulders (elements) with a minimum areal extent and subtle relief. Linearity is not included within the ontology, as whilst the patterned ground can be broadly linear in form, the upslope ends of these features merge into polygonal arrangements, and bifurcations of stripes are common. Boulders are delineated using spectral characteristics derived from either true

colour (red, green, blue - RGB) or near-infrared (NIR) false-colour composite imagery. The extent to which it is possible to apply this ontology to extract patterned ground from positions of boulders, across different resolution imagery, including datasets produced using SfM, is one of the challenges addressed within this paper.

Datasets

A series of different datasets have been used within this paper, including existing imagery and topographic data, and newly-acquired UAV surveys (Fig. 3 and Table 1). Three sets of pre-georeferenced aerial photos (two true-colour RGB and one false-colour infrared) were obtained from Dartmoor National Park Authority (DNPA) and Devon County Council (DCC). The ground resolution of the true-colour RGB imagery datasets are 25 cm and 12.5 cm, while the false-colour infrared imagery has a resolution of 12.5 cm. LiDAR data collected in 2013 was obtained from the TellusSW programme at 1 m resolution (Ferraccioli et al., 2014).

Two new surveys were flown during the summer of 2016 using two different platforms: a SenseFly EBEE fixed-wing UAV and a DJI Phantom3 Professional rotary-wing UAV. In both cases flights were pre-planned to ensure 80% endlap and 85% sidelap, providing maximal overlap between adjacent images for optimal SfM analysis. This degree of overlap was based on experimentation from previous missions and the recommendation of the flight planning software. The flight mission planning software used was eMotive for the Ebee and Pix4DCapture for the DJI Phantom. The EBEE was equipped with an 18.2 MP RGB camera, with automatic image capture every three seconds on pre-planned flight lines, and a total of 219 images were collected across a 0.42 km^2 survey area. The Phantom3 Pro UAV was equipped with a 12.4 MP RGB camera with a 35 mm equivalent lens, and captured two hundred images across a 0.12 km^2 area. The ground sampling distance of the two surveys were 3.6 cm (EBEE) and 2.3 cm (Phantom3). Each mission took <20mins flight time.

Data Processing

Post-processing of both sets of UAV data was undertaken using Pix4DMapper Pro for the generation of seamless orthomosaic imagery and DSM.

All imagery and topographic surfaces were clipped to a 0.35 km^2 area (Fig. 1) to reduce processing time. An unsupervised classification was run on each set of imagery data, using the three colour bands (R-G-B/NIR-R-G) as the input for each image. The unsupervised classification undertakes cluster analysis on the dataset, and the resulting dendrogram is then cut to return a specified number of classes. Experimentation showed that ten classes were sufficient to differentiate boulders within the imagery. The output of unsupervised classification was reclassified to retain only those classes that represented boulders. These

were then generalised to patterned ground by converting 'boulder' classes to polygons, which were then aggregated based on a distance threshold. Following experimentation with difference threshold distances, adjacent boulders within 0.5 m of each other were considered part of the same landform, and the feature retained if it had an area of at least 4 m^2. Elevational cross-sections were extracted from each of the three DSMs (LiDAR, EBEE DSM and DJI Phantom DSM) across a single stripe.

Results

1) Spectral signature and recognition of landform planform

Unsupervised classification of imagery in all cases delineates the key features on the ground, and patterns derived from classification are superficially similar across all datasets (Fig. 4). A notable difference between classified outputs is the 'blockiness' of the delineated features: the Phantom3 UAV imagery data produces very fine-grained output (Fig 4B) whilst the 2005/6 25cm resolution vertical RGB imagery produces more 'continuous' groups of boulders (Fig 4A). The differences between the DNPA RGB and NIR outputs, both of which have a spatial resolution of 12.5 cm, are striking (Figs 4C and 4D). The output from NIR imagery produces 'fuller' mapping and more continuous clustering of boulders than the output from RGB imagery, in spite of having been collected contemporaneously and at the same resolution. This can likely be attributed to the ability of the NIR band to better discriminate between boulder and vegetation cover than RGB imagery as a result of the clear spectral response produced by strong absorption of red and strong reflectance of NIR by vegetation (e.g. Walker et al 2011).

[insert Figure 4]

Examination of a single stripe of patterned ground demonstrates the impact of different surveys on the results at the element (boulder) level (Figs 5 and 6). The unsupervised classification approach applied to the highest resolution survey (the Phantom3 imagery) discriminates all boulders including those with a long axis as small as 0.1 m. The processing of this dataset has excluded any boulders with a mapped area smaller than 0.05 m^2 (~0.22 m x 0.22 m in size), and aggregation of the unsupervised imagery output identifies boulder stripes that closely resemble the true spatial extent of these features. Individual boulders are not clearly differentiated on the 12.5 cm NIR imagery, and as a consequence the mapped output is fuzzier than the output produced using the other three datasets, with stone stripes consequently depicted as wider features (Fig 6), although again the position of the feature is broadly correct.

[insert Figure 5]

[insert Figure 6]

2) DEMs and landform long and cross-profile topographic signatures

Here comparison is made between the airborne LiDAR data and DSMs produced by SfM applied to both the Phantom3 and EBEE-derived images (Figs 7 and 8). In Figure 7 both topography and angle of slope have been extracted and the extent of the stone stripe (produced based upon the NIR and the Phantom3 UAV surveys) given. The resolution differences between the LiDAR (1 m resolution) and much higher-resolution SfM DSMs are clear and apparent in the contouring (Fig. 4); however, both UAV surveys produce the same topographic patterns. Slope angles are also broadly aligned for the UAV surveys, but show the local 'noise' generated by mapping of individual boulder edges within the surveys (Fig 7). Smoothing these data using 1 m-long moving averages show that the single stripe examined occupies slopes of ~<10-12 degrees. For both slope and elevation, the same (albeit coarser) trends are captured across transect V-W by the LiDAR dataset, with the stripe of patterned ground occupying a slope of ~5-10 degrees (as measured at 1 m resolution).

[insert Figure 7]

[insert Figure 8]

The cross-sectional transect X-Y demonstrates the key difference between the high-resolution LiDAR DTM and the ultra-high-resolution UAV-SfM DSM (Fig 8): it is not possible to discriminate any topographic expression of the stone stripe in the LiDAR dataset. Both UAV-SfM DSMs show the same pattern, forming a negative topographic feature, with a relief of ~0.15-0.2 m, a topography that is confirmed from the ground (Fig 2D). Although transect V-W is very similar for both the EBEE and the Phantom3 DSM outputs, more detail is captured in the EBEE DSM, even though it has a marginally coarser resolution.

Discussion

The combination of UAV, SfM and automated mapping technologies offer potential for enhanced analysis of geomorphological features. Here we consider the experience of using these approaches to analyse low relief and relict periglacial landforms and consider the scope for wider application. We examine the capability of both spectral signature and DEM generation from SfM in the analyses of these landforms at the Leeden Tor site on Dartmoor, and offer recommendations on applications of these methodologies, as summarised in Fig. 9.

[insert Figure 9]

1) Use of Spectral signature - RGB and NIR

Although spectral signature has been used to identify the nature and extent of active permafrost-related periglacial features by using patterns of vegetation (e.g. Allen et al 2008, Ulrich et al 2009, Poelking et al 2015) it has rarely been considered for the identification of patterned ground. In the study presented here the spectral signature provides a powerful tool for visually identifying the landform elements (boulders) that constitute and define the recognisable landforms (sorted patterned ground). For these relict features both RGB and NIR work well due to the vegetation versus 'bare rock' characteristics of the boulders (Figs 2 and 3). Both the resolution and processing of the data (i.e. how the elements are grouped into a landform at the automated classification stage) will determine the apparent clarity of visual expression of the landform features. Applying the same ontology across the different data sets suggests that the resolution of the imagery has some impact on the perceived structure (stripes and polygons) of the patterned ground (Fig 4), where structure is in general visually most defined for the coarser imagery (Fig 4C,D) and NIR (Fig 4D). In contrast, at the element level the higher resolution imagery is the most informative (Fig 5). In the analyses of polygenetic, relict features such as those presented here, data on boulder size, and orientation of long axis may be significant in understanding processes of landform formation. These data can be extracted from the highest resolution drone imagery (Fig. 5) which is superior to the available lower resolution, aerial imagery (Table 1) which is more suitable at the larger landform (patterned ground) scale of analysis. The resulting processed imagery is well suited to manually identifying the basic structure (e.g. stripe versus polygon) observed within the patterned ground (compare Fig 3 and Fig 4). In order to automate the mapping of the different structures that can be observed manually, further consideration would need to be applied to the nature of element to landform amalgamation at the processing level. What is clear from the UAV imagery is the high quality and resolution of the imagery available (Fig. 5). In remote areas, where many active periglacial environments are found, this quality of the UAV RGB imagery means that many smaller landforms and landform elements that currently go unrecognised on coarser commercially available (aerial/satellite) imagery could potentially be identified. The presence of such landforms are often significantly underestimated when using coarser data sets (Dąbski et al. 2017) and yet identification of these smaller features can prove crucial in periglacial environments as they record landscape response to a changing climate (Lemke et al 2007; Dąbski et al. 2017).

2) LiDAR versus SfM generated DEMs

Long profile and cross-sectional data extracted from the SfM DEM from the Leeden Tor study shows clear pattern reproducibility between the UAV surveys (Figs 7 and 8). In comparison to the airborne LiDAR survey data it is clear that the produced DEM slopes are scale dependent (Fig 8) and thus the low relief topography in cross-section is clearly identifiable on the higher resolution UAV imagery, but not on the coarser LiDAR data (Fig. 8). This reinforces earlier research demonstrating scale dependencies in estimation of slope (e.g. Zhang et al 1999; Goodchild 2011), whereby as resolution decreases so slopes get lower. According to Zhang et al. (1999) the optimal DEM resolution for geomorphic analysis should be the finest available to the researcher. In the case of the ultra-high resolution SfM DEM slope data can reflect boulder edges, and hence the problem may not be that of downscaling DEMs (*sensu* Luoto and Hjort 2008) but identifying an appropriate scale to re-sample DEMs in order to extract useful data for generalising the patterned ground properties.

A significant consideration in determining whether a SfM-derived DEM is suitable for landform analysis is the aim of the survey – is this to produce a DTM or DSM? For most landform studies we are interested in the landform surface (thus a DTM is optimal), which means that SfM may not be an option in heavily vegetated areas. Most active periglacial and recently de-glaciated areas are thus prime targets for SfM due to their lack of vegetation cover, which means that SfM performed on UAV and aerial imagery can offer a cost-effective and higher resolution alternative to LiDAR (Fig. 9), depending on the spatial extent of the area of interest. However, when investigating relict periglacial features, vegetation can become problematic. In this respect careful consideration should be given to when a drone survey is undertaken due to weather conditions etc. (e.g. Duffy et al 2017). On Dartmoor the optimal time for survey would be Spring when weather conditions (clarity and wind) are optimal for flying and prior to the significant growth of bracken, which can grow to 1 m in height and thus in some areas may mask subtle topographic features, or even exacerbate them if it grows in the soil rich, inter-stone-rich areas. Our UAV surveys were undertaken in August of 2016 when bracken growth is still relatively high (but dying back). However the selected sites are dominantly grass covered and well grazed (Fig 2) minimising seasonal variations. Despite this, surface-enhancing effects of the vegetation (in the order of +20cm) are still visible in the last few metres of the example long profile in Fig. 7 (10.5-13.5m along the profile). Vegetation cover, then, should be an important consideration depending on the level of accuracy required and the intended purpose of the survey.

Scale should also be considered when selecting the approach for DEM generation. For very small (<m-scale) landform elements (such as boulders) SfM from ground-based imagery may be suitable (e.g. Kääb et al 2014). For landform elements that cover an extended area and intermediate sized landform features (<km) UAV based SfM is typically more suitable and rivals ground based LiDAR, however for larger (ha) landform features extending across large areas UAV based data becomes less useful and SfM applied to aerial photography from manned aircraft or LiDAR data may be optimal (Fig 9).

3) Prospects for SfM and Spectral Signature -

A combination of SfM-derived DEM and spectral signature provides a potentially powerful tool for the analysis of landforms from a UAV platform. Off-the shelf drones such as those used in this study are capable of creating imagery of sufficient quality for efficient and rigorous landform analysis, particularly where backed up by accurate ground control points. Where spectral contrasts exist for the landforms being analysed, such as the bare rock and vegetation at Leeden Tor, automated processing of RGB images provides a useful way of delimiting elements in the landscape which could then be used for further detailed analysis (e.g. in the case of the boulder elements this could be long axis orientation, size segregation etc.) depending on the resolution of the imagery. In areas of minimal vegetation cover SfM can be used to effectively analyse the geomorphology of landforms from repeat survey. Whilst this can be achieved on the ground for larger (0.5 km^2) areas (Piermattei et al., 2016), the processing time currently is a major limitation, although this should improve as computer systems become more powerful and software more efficient. It may not always be possible to obtain suitable imagery from the ground, making a UAV a valuable extension of the geomorphologists tool-box. The georeferenced images and overlap minimise processing time, maximise accuracy and improve coverage. This then enables the UAV camera platform to provide superior imagery for SfM-DEM processing, providing a viable alternative to LiDAR for intermediate-sized field areas (Fig.9). For subtle relief features, such as those investigated here, the higher resolution offered by SfM from UAV data (and potentially from aerial images for larger areas) proved superior to available LiDAR on which the features cannot be observed (Fig 8). For recognising the planform structure of the patterned ground automated processing of the RGB/NIR imagery was most effective at the coarser scales (Fig. 4), which also enables coverage of larger areas. This approach would be less useful for observation of active patterned ground due to more limited vegetation contrast.

Whilst this study has been targeted at a relict periglacial environment now present within a northern hemisphere, oceanic climate zone, the workflow proposed here could potentially be applied successfully to other geoscience applications and environments. The prerequisites

for suitable settings would be study areas where the features of interest have sufficient spectral contrast to optimise landscape element recognition and limited vegetation cover to maximise DSM accuracy. This might include for example dryland environments where there is scope to develop this approach for mapping features in Quaternary palaeoflood deposits to enable palaeoflood reconstruction (e.g. catastrophic boulder deposits reported from alluvial fans of the Atacama Desert of Northern Chile by Mather & Hartley 2005, supplemented with palaeo-hydrology approaches such as those presented by Stokes et al 2012 and Mather & Stokes 2016) or the mapping of gully-scale soil erosional features (such as the visually contrasting grassland gully system features described by Telfer et al 2014 from the Drakensberg foothills of Rooiberge, South Africa).

Conclusions

Recognition of relict periglacial landform features can be greatly enhanced by automated mapping using spectral 2D imagery. The recognition of elements of <1 m is maximised from the highest resolution imagery (UAV RGB) whilst recognition of the landform (10-100 m scale) is maximised on coarser resolution and NIR aerial imagery. Topographic metrics of these low relief landform features can be best extracted using SfM-processed UAV imagery, and in this case airborne LiDAR data proved to be less effective for this purpose. Integrating these approaches provides a powerful tool for rapid reconnaissance of large areas of such features, facilitating the extraction of meaningful topographic and spatial data that can inform on the origin of relict landforms. It is however, essential to match the scale of features under consideration to the appropriate scale of datasets available. This approach has applications for mapping topographically subtle but spectrally distinct geomorphic features in other environments with limited vegetation cover (eg deserts or grasslands).

References

Abermann J, Fischer A, Lambrecht A and Geist T (2010) On the potential of very high-resolution repeat DEMs in glacial and periglacial environments. *The Cryosphere* 4: 53-65

Allen S, Owens I and Huggel C (2008) A first estimate of mountain permafrost distribution in the Mount Cook Region of New Zealand's southern Alps. In: *9th International Conference on Permafrost , Fairbanks, Alaska*, 29 June 2008 – 03: 37- 42

Bennett MR, Mather AE and Glasser, NF (1996) Earth hummocks and boulder runs at Merrivale, Dartmoor, In: Charman, DJ, Newnham RW, Croot DW (Eds), *Devon and East Cornwall: Field Guide*, Quaternary Research Association, London, 81–96

Boulton SJ and Stokes M (2018) Which DEM is best for analysing fluvial landscape development in mountainous terrains? *Geomorphology* 310: 168-187

Bradley R. (2000) *An archaeology of natural places*. Routledge, London

Carrivick JL, Smith, MW and Quincey DJ. (2016) *Structure from Motion in the Geosciences*, Wiley-Blackwell, Chichester, UK, 208 pp.

Chiverrell RC and Thomas, GSP (2010) Extent and timing of the Last Glacial Maximum (LGM) in Britain and Ireland: a review, *Journal of Quaternary Science*, 25 (4): 535-549

Dąbskia M, Zmarzb A, Pabjanekb P, Korczak-Abshirec M, Karszniab I and Chwedorzewskac, KJ (2017) UAV-based detection and spatial analyses of periglacial landforms on Demay. Point (King George Island, South Shetland Islands, Antarctica). *Geomorphology* 290: 29-38.

De Haas T, Kleinhans MG, Carbonneau PE, Rubensdotter L and Hauber E (2015) Surface morphology of fans in the high-Arctic periglacial environment of Svalbard: Controls and processes. *Earth Science Reviews* 146: 163-182

Drăguţ L and Blaschke T (2006) Automated classification of landform elements using object-based image analysis. *Geomorphology* 81: 330-344.

Duffy JP, Cunliffe AM, DeBell L, Sandbrook C, Wich AA, Shutler JD, Myers-Smith IH, Varela, MR and Anderson K (2017) Location, location, location: considerations when using lightweight drones in challenging environments. *Remote Sensing in Ecology and Conservation*. DOI: 10.1002/rse2.58

Ebdon M (2014). *The Turnpike roads of Devon in 1840*. ISBN 978-0-9930072-0-0. 101pp

Ely JC, Graham C, Barr ID, Rea BR, Spagnolo M and Evans J (2016) Using UAV acquired photography and structure from motion techniques for studying glacier landforms: application to the glacial flutes at Isfallsglaciären, *Earth Surface Processes and Landforms* 42: 877-888

Evans DJA, Harrison S, Vieli A and Anderson E (2012a) The glaciation of Dartmoor: the southernmost independent Pleistocene ice cap in the British Isles, *Quaternary Science Reviews* 45: 31-53

Evans DJA, Harrison S, Vieli A. and Anderson E (2012b) Dartmoor's overlooked glacial legacy, *Geology Today*,28 (6): 224-229

Evans DJA, Ewertowski M and Orton, C (2016) Fláajökull (north lobe), Iceland: active temperate piedmont lobe glacial landsystem. *Journal of Maps* 12: 777-789.

Evans DJA, Kalyan R and Orton C (2017) Periglacial geomorphology of summit tors on Bodmin Moor, Cornwall, SW England, *Journal of Maps* 13 (2): 342-349

Evans IS (2012) Geomorphometry and landform mapping: what is a landform? *Geomorphology* 137: 94-106

Ferraccioli F, Gerard F, Robinson C, Jordan T, Biszczuk M, Ireland L, Beasley M, Vidamour, A, Barker A, Arnold R, Dinn M, Fox A and Howard A (2014) *LiDAR based Digital Terrain Model (DTM) data for South West England.* NERC Environmental Information Data Centre https://doi.org/10.5285/e2a742df-3772-481a-97d6-0de5133f4812

Fleming A (2008) *The Dartmoor Reaves: investigating prehistoric land division*. Windgather, Oxford.

Fonstad, MA, Dietrich JT, Courville BC, Jenson JL and Carbonneau PE (2013). Topographic structure from motion: a new development in photogrammetric measurement. *Earth Surface Processes and Landforms* 38: 421-430

Gerrard J (1988) Periglacial modification of the Cox Tor-Staple Tors area of western Dartmoor, England, *Physical Geography* 9 (3): 280-300

Giles PT (1998) Geomorphological signatures: classification of aggregated slope unit objects from digital elevation and remote sensing data. *Earth Surface Processes and Landforms* 23: 581-594.

Gómez-Gutiérrez A, de Sanjosé-Blasco JJ, de Matias-Bejarano J and Berenguer-Sempere, F (2014) Comparing Two Photo-Reconstruction Methods to Produce High Density Point Clouds and DEMs in the Corral del Veleta Rock Glacier (Sierra Nevada, Spain), *Remote Sensing* 6 (6): 5407-5427

Goodchild MF (1987) A spatial analytical perspective on geographical information systems. *International Journal of Geographical Information Systems* 1: 327-334.

Goodchild MF (2011) Scale in GIS: an overview, *Geomorphology* 130: 5-9.

Gunnell Y, Jarman D, Braucher R, Calvet M, Delmas M, Leanni L, Bourlès D, Arnold M, Aumaître G and Keddaouche K (2013) The granite tors of Dartmoor, Southwest England: rapid and recent emergence revealed by Late Pleistocene cosmogenic apparent exposure ages. *Quaternary Science Reviews* 61: 62-76

Immerzeel WW, Kraaijenbrink PDA, Shea JM, Shrestha AB, Pellicciotti F, Bierkens MFP and de Jong SM (2014) High resolution monitoring of Himalayan glacier dynamics using unmanned aerial vehicles, *Remote Sensing of Environment* 150: 93-103

James HCL (2004) Evidence for the extent of permafrost activity in south west England during the last cold stage, *Geoscience in south-west* England 11: 37-41

Kääb A, Girod L and Berthling I (2014) Surface kinematics of periglacial sorted circles using structure-from-motion, *The Cryosphere* 8: 1041-1056

Kršák B, Blištan P, Pauliková A, Puškárová P, Kovanič L, Palková J and Zelizňaková V (2016) Use of low-cost UAV photogrammetry to analyze the accuracy of a digital elevation model in a case study. *Measurement* 91: 276-287.

Lemke P, Ren J, Alley RJ, et al.: 2007.Observations: Changes in Snow, Ice and Frozen Ground, in: *Climate Change 2007, The Physical Science Basis, Contribution of Working Group I to the Fourth Assessment Report of the Intergovernmental Panel on Climate Change, edited* by: Solomon, S. Qin D, Manning M. et al., Cambridge University Press, Cambridge, United Kingdom and New York, NY, USA.

Lucieer A, de Jong SM and Turner D (2013) Mapping landslide displacements using Structure from Motion (SfM) and image correlation of multi-temporal UAV photography, *Progress in Physical Geography* 38 (1): 97-116

Louto M and Hjort J (2008) Downscaling of coarse-grained geomorphological data, *Earth Surface Processes and Landforms* 33: 75-89.

MacMillan RA and Shary PA (2009) Landforms and Landform Elements in Geomorphometry. In: Hengl T and Reuter H (Eds.), 2009. *Geomorphometry: Concepts, Software, Applications. Developments in Soil Science* 33. Elsevier, Amsterdam. 227-254

Mancini F, Dubbini M, Gattelli M, Stecchi F, Fabbri S and Gabbianelli G (2013) Using Unmanned Aerial Vehicles (UAV) for High-Resolution Reconstruction of Topography: The

Structure from Motion Approach on Coastal Environments, *Remote Sensing* 5 (12):z 6880-6898

Martha TR, Kerle N, Jetten V, van Westen CJ and Kumar KV (2010) Characterising spectral, spatial and morphometric properties of landslides for semi-automatic detection using object-oriented methods. *Geomorphology* 116: 24-36.

Mather AE and Hartley AJ (2005) Flow Events on a hyper-arid alluvial fan: Quebrada Tambores, Salar de Atacama, northern Chile. In: Harvey AM, Mather AE and Stokes M. (eds) *Alluvial Fans: Geomorphology, Sedimentology, Dynamics*. Geology Society Special Publication 251, London, 9-29

Mather AE and Stokes M (2016) Extracting palaeoflood data from coarse-grained Pleistocene river terrace archives: an example from SE Spain. *Earth Surface Processes and Landforms* 41**:** 1991-2004.

Micheletti N, Chandler JH and Lane SN (2015a) Structure from motion (SFM) photogrammetry, in: Clarke, L.E. & Nield, J.M. (Eds.), *Geomorphological Techniques*, British Society for Geomorphology, London, Chap. 2, Sec. 2.2

Micheletti N, Chandler JH and Lane SN (2015b) Investigating the geomorphological potential of freely available and accessible structure-from-motion photogrammetry using a smartphone, *Earth Surface Processes and Landforms* 40: 473-486

Nolan M, Larsen C and Sturm M (2015) Mapping snow depth from manned aircraft on landscape scales at centimeter resolution using structure-from-motion photogrammetry. *The Cryosphere* 9: 1445-1463

Palmer JA and Neilson RA (1962) The origin of granite tors on Dartmoor, Devonshire, *Proceedings of the Yorkshire Geological Society* 33: 315-339

Piermattei L, Carturan L, de Blasi F, Tarolli P, Dalla Fontana G, Vettore A and Pfeifer N (2016) Suitability of ground-based SfM-MVS for monitoring glacial and periglacial processes, *Earth Surface Dynamics* 4: 425-443

Poelking EL, Schaefer CER, Fernandes Filho EI, de Andrade AM and Spielmann AA (2015) Soil–landform–plant-community relationships of a periglacial landscape on Potter Peninsula, maritime Antarctica. *Solid Earth* 6: 583-594

Ryan JC, Hubbard AL, Box JE, Todd J, Christoffersen P, Carr JR, Holt TO and Snooke, N (2015) UAV photogrammetry and structure from motion to assess calving dynamics at Store Glacier, a large outlet draining the Greenland Ice Sheet. *The Cryosphere* 9: 1-11

Santangelo M, Marchesini I, Bucci F, Cardinali M, Fiorucci F and Guzzetti F (2015) An approach to reduce mapping errors in the production of landslide inventory maps. *Natural Hazards and Earth System Sciences* 15: 2111-2126

Smith MW, Carrivick JL and Quincey DJ (2016) Structure from motion photogrammetry in physical geography, *Progress in Physical Geography* 40 (2): 247-275

Smith MW, Carrivick JL, Hooke J and Kirkby MJ (2014) Reconstructing flash flood magnitudes using 'Structure-from-Motion': A rapid assessment tool. *Journal of Hydrology* 518 (Part B): 1914-1927

Stokes M, Griffiths JS and Mather AE (2012) Palaeoflood estimates of Pleistocene coarse grained river terrace landforms (Rio Almanzora, SE Spain). *Geomorphology* 149: 11-26

Te Punga MT (1956) Altiplanation terraces in southern England. *Biuletyn Periglacjalny* 4: 331–338

Telfer, MW, Mills SC and Mather, AE (2014). Extensive Quaternary aeolian deposits in the Drakensberg foothills, Rooiberge, South Africa. *Geomorphology* 219: 161-175.

Telfer MW, Fyfe RM and Lewin S (2015) Automated mapping of linear dunefield morphometric parameters from remotely-sensed data. *Aeolian Research* 19: 215-224.

Tilley C, Hamilton S, Harrison S and Anderson E (2000) Nature, Culture, Clitter: Distinguishing Between Cultural and Geomorphological Landscapes; The Case of Hilltop Tors in South-West England, *Journal of Material Culture* 5 (2): 197-224

Tonkin TN, Midgley NG, Graham DJ and Labadz JC (2014) The potential of small unmanned aircraft systems and structure-from-motion for topographic surveys: A test of emerging integrated approaches at Cwm Idwal, North Wales. *Geomorphology* 226: 35-43

Ulrich M, Grosse G, Chabrillat S and Schirrmeister L (2009) Spectral characterization of periglacial surfaces and geomorphological units in the Arctic Lena Delta using field spectrometry and remote sensing. *Remote Sensing of Environment* 113: 1220-1235.

Walker DA, Kuss P, Epstein HE, Kade AN, Vonlanthern CM, Raynolds,MK and Daniëls FJA (2011) Vegetation of zonal patterned-ground ecosystems along the North America Arctic bioclimate gradient. *Applied Vegetation Science* 14: 440-463.

Waters RS (1964) The Pleistocene legacy to the geomorphology of Dartmoor, In: Simmons, I.G. (Ed.), *Dartmoor Essays*, Devonshire Association for the Advancement of Science, Exeter, pp. 73-96

Westoby MJ, Brasington J, Glasser NF, Hambrey MJ and Reynolds JM (2012) 'Structure-from-Motion' photogrammetry: A low-cost, effective tool for geoscience applications, *Geomorphology* 179: 300-314

Westoby MJ, Dunning SA, Woodward J, Hein AS, Marrero SM, Winter K and Sugden DE (2015). Sedimentological characterization of Antarctic moraines using UAVs and Structure-from-Motion photogrammetry, *Journal of Glaciology* 61: 1088-1102

Zhang X, Drake NA, Wainwright J and Mulligan M (1999) Comparison of slope estimates from low resolution DEMs: scaling issues and a fractal method for their solution, *Earth Surface Processes and Landforms* 24: 763-779.

Figure captions

Fig. 1: Location of Leeden Tor within Dartmoor National Park and the UK. The ordnance survey map (© Crown copyright and database rights 2017 Ordnance Survey: Digimap Licence) shows spatial extent of prehistoric field boundaries and hut circles also evident in the aerial imagery (Figure 3). Box on topographic map indicates survey area.

Fig. 2: Field site from UAV (DJI Phantom 3 Professional) aerial and field shots. A) oblique aerial UAV image of study area and boulder runs. Note tor-less nature of study site. Dartmoor ponies (solid arrow) for scale and 2 persons and dog (circled) . B) overhead UAV shot (2 persons and dog top left as reference from (A). C) field shot of positive relief of hut circle and D) field shot of subtle negative relief of patterned ground (polygonal in foreground to more linear in background).

Fig. 3: Aerial imagery of Leeden Tor from five different imagery datasets (A-E) and 3.5 cm resolution hillshaded DSM derived from EBEE UAV (F). A: EBEE RGB orthomosaic (3.6 cm resolution); B: Phantom UAV RBG orthomosaic (2.3 cm resolution); C: DNPA RGB imagery (12.5 cm resolution); D: DNPA NIR imagery (12.5 cm resolution); E: GeoPerspectives RBG imagery (25 cm resolution, copyright GeoPerspectives). Circular features in the southern (bottom right) part of the images are prehistoric round houses. Box on panel F indicates location of feature shown in Figures 5 and 6.

Fig. 4: Planform of patterned ground across Leeden Tor derived from unsupervised classification and aggregation of features from four sets of imagery data. Contours lines are set at 25 cm intervals. A: 25 cm resolution GeoPerspectives RGB imagery; contours derived from LiDAR. B: 2.6 cm resolution RGB Phantom UAV; contours derived from Phantom UAV DSM. C: 12.5 cm resolution DNPA RGB imagery; contours derived from LiDAR. D: 12.5 cm resolution DNPA NIR imagery; contours derived from LiDAR.

Fig. 5: RGB imagery derived from Phantom UAV at 2.3 cm resolution (A); vectorised position of boulders though reclassification of RGB imagery, with grey indicating < 0.05 m2 (B); generalised location of stripe and 25 cm contours from Phantom UAV-derived DTM (C). X-Y and V-W indicates locations of topographic cross section (Figures 7 and 8).

Fig. 6: false-colour IR imagery derived from aerial survey at 12.5 cm resolution (A); vectorised position of boulder spreads though reclassification of false-colour IR imagery, with three classes associated with boulders (B); generalised location of stripe and 25 cm contours from TELLUS SW LiDAR survey (C). X-Y and V-W indicates locations of topographic cross section (Figures 7 and 8).

Fig. 7: Long profile V-W through stripe illustrated in Figures 5 and 6, showing elevation derived from LiDAR, Phantom UAV DSM and EBEE UAV DSM (upper panel), derived slope angles from UAV DSMs (middle panel) and LiDAR-derived slope and 1 m moving-average slopes from UAV DSMs (lower panel).

Fig. 8: Cross section X-Y across boulder stripe illustrated in Figures 5 and 6, showing elevation derived from LiDAR, Phantom UAV DSM and EBEE UAV DSM.

Fig. 9: Suggested appropriate approaches to landform analysis based on available/acquired datasets for DEM and/or Spectral analysis of landforms. For Satellite based data - Optical = imagery e.g. Landsat; SAR = Synthetic Aperture Radar. Underlined text in lighter shaded boxes indicates resources and approaches used in this study.

Table 1: details of datasets utilised at Leeden Tor

Dataset	Resolution	Date of acquisition	Source
RGB geotiff imagery	25 cm	Autumn/Winter 2006	Devon CC (copyright GeoPerspectives)
RGB geotiff imagery	12.5 cm	April 2015	DNPA
False-colour IR imagery	12.5 cm	April 2015	DNPA
LiDAR DTM	100 cm	July 2013	TELLUS SW
RGB geotiff imagery and DSM	3.6 cm	August 2016	EBEE UAV (UoP)
RGB geotiff imagery and DSM	2.3 cm	September 2016	Phantom UAV (UoP)

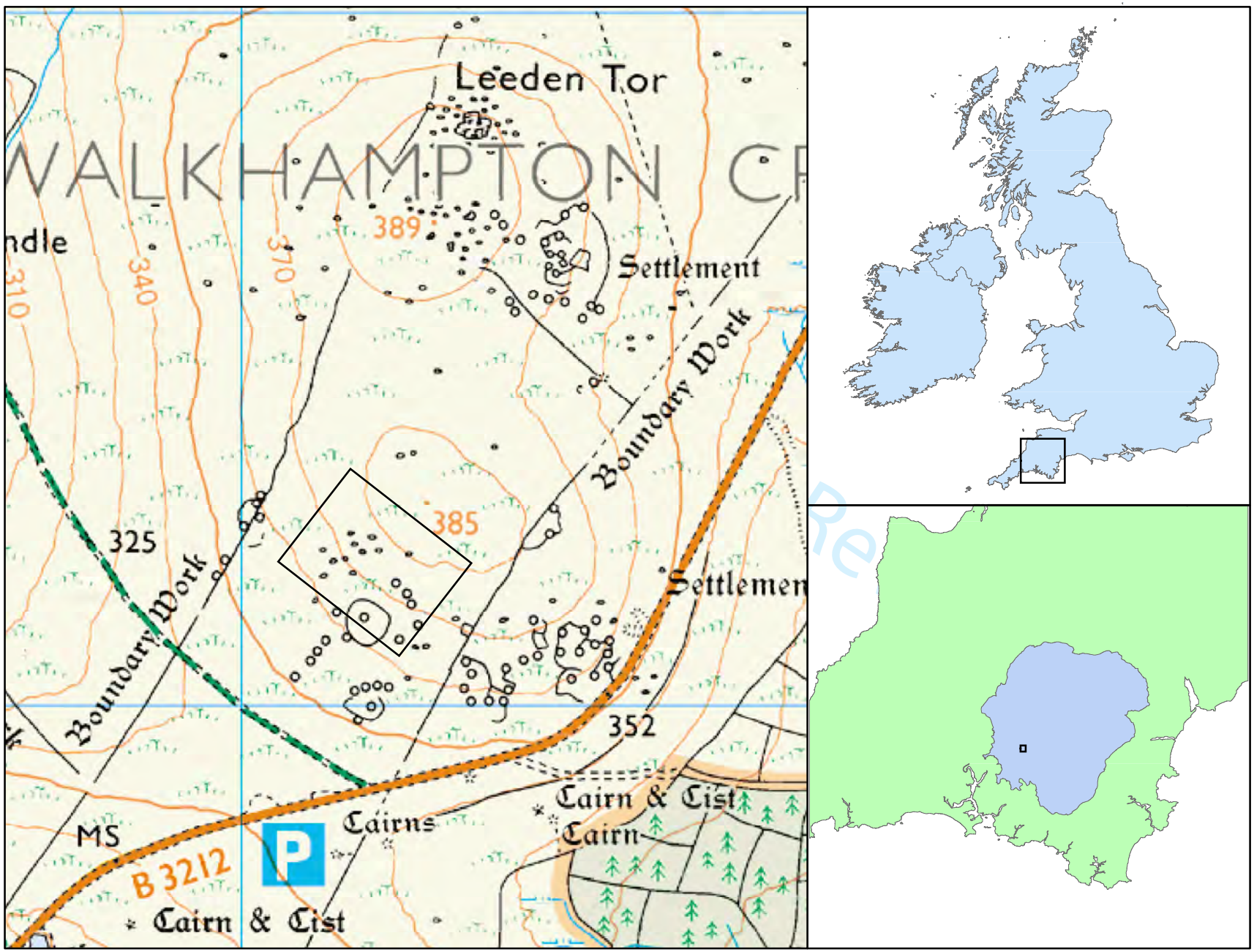
Leeden Tor
WALKHAMPTON CR
ndle
389
370
340
310
Settlement
Boundary Work
385
325
Boundary Work
Settlemen
352
Cairn & Cist
Cairns
Cairn
MS
B 3212
P
Cairn & Cist

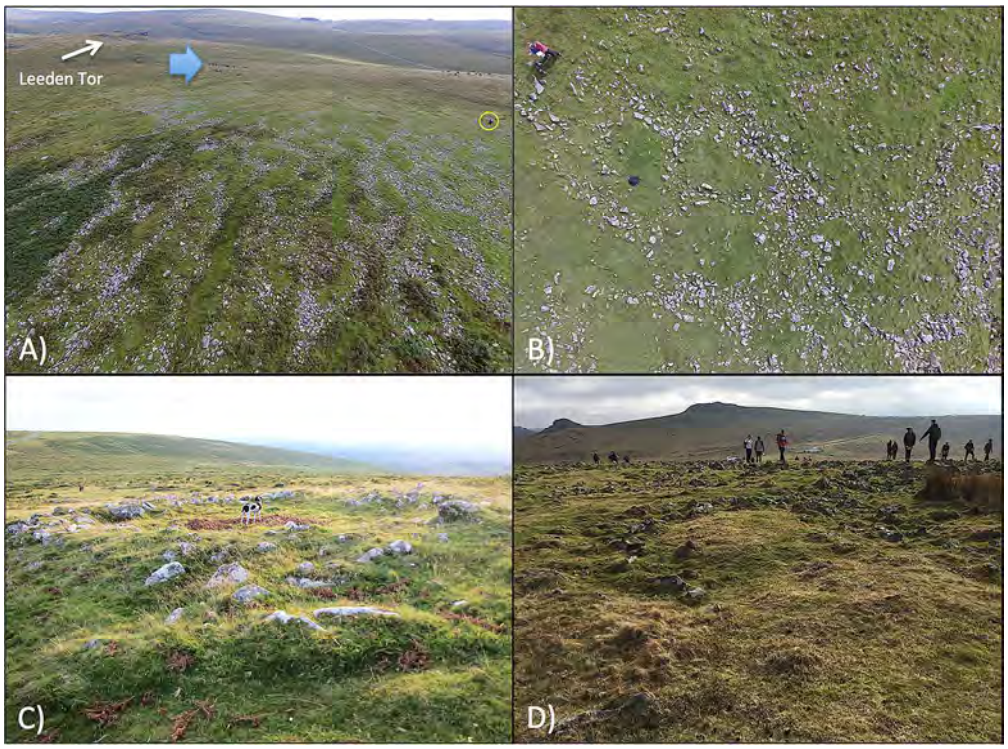

199x147mm (300 x 300 DPI)

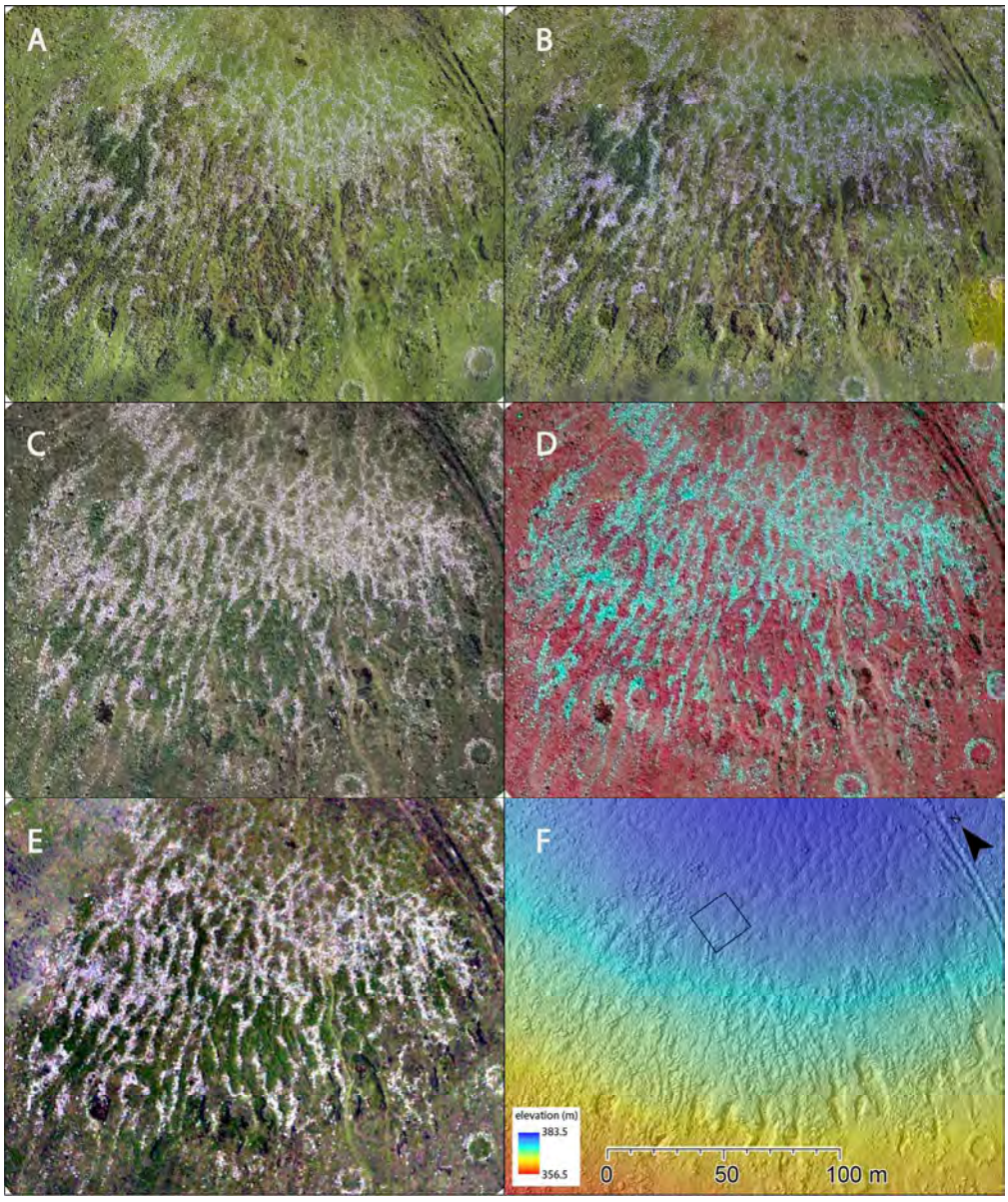

172x204mm (300 x 300 DPI)

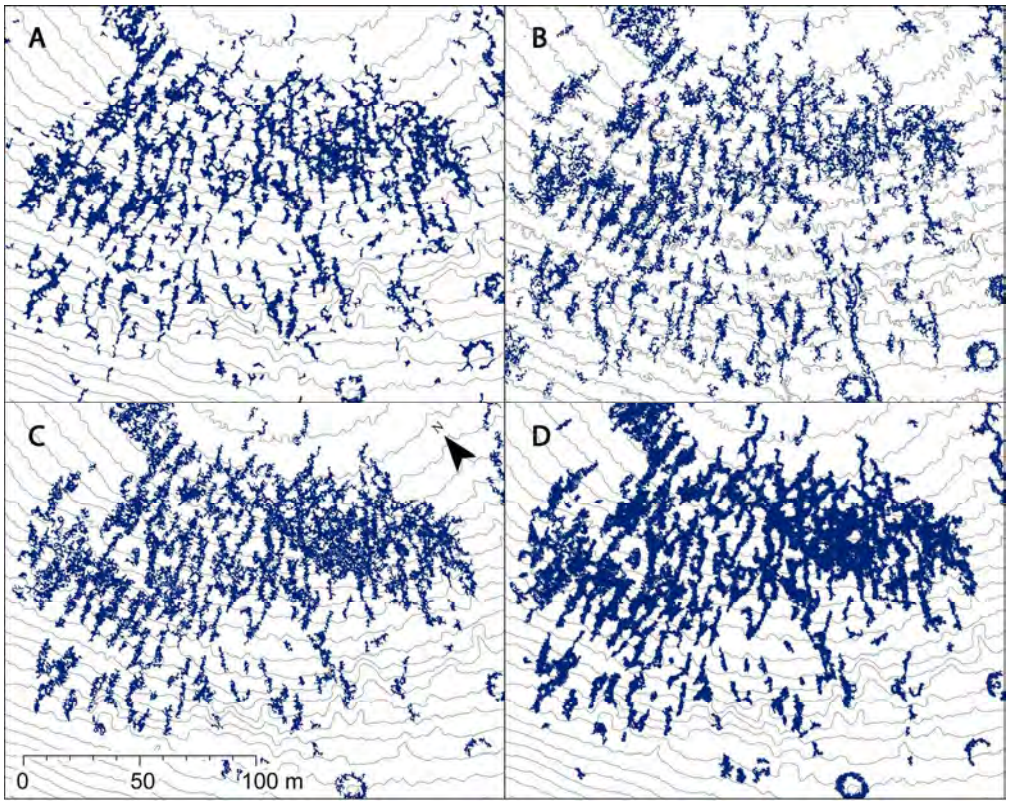

136x108mm (300 x 300 DPI)

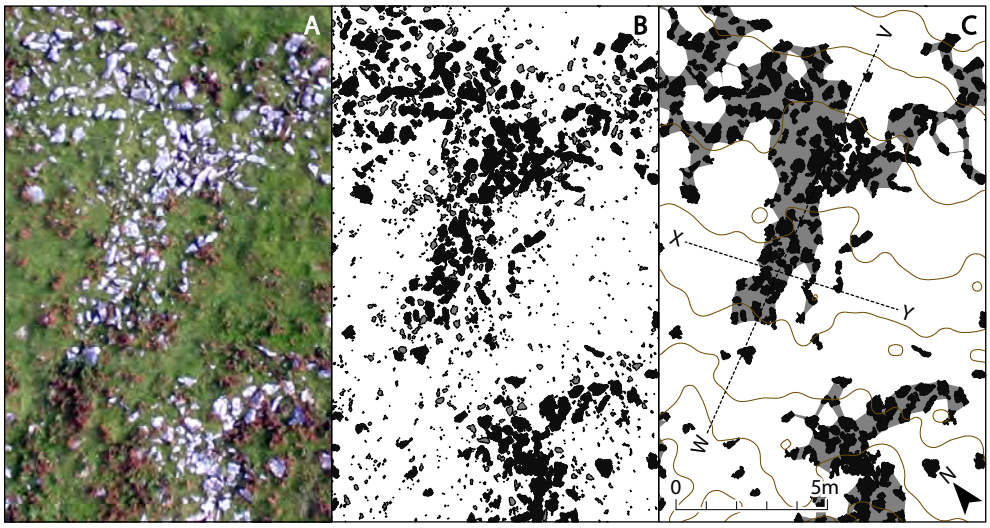

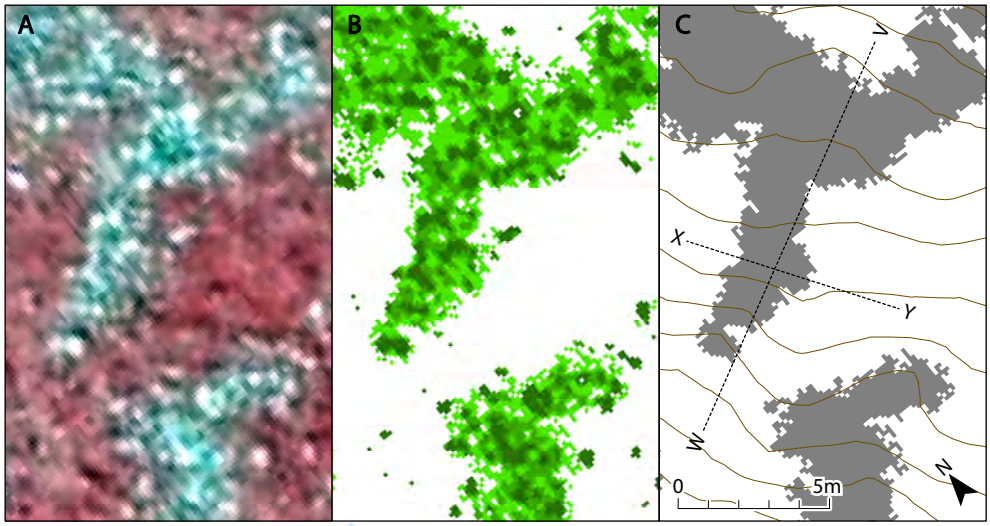

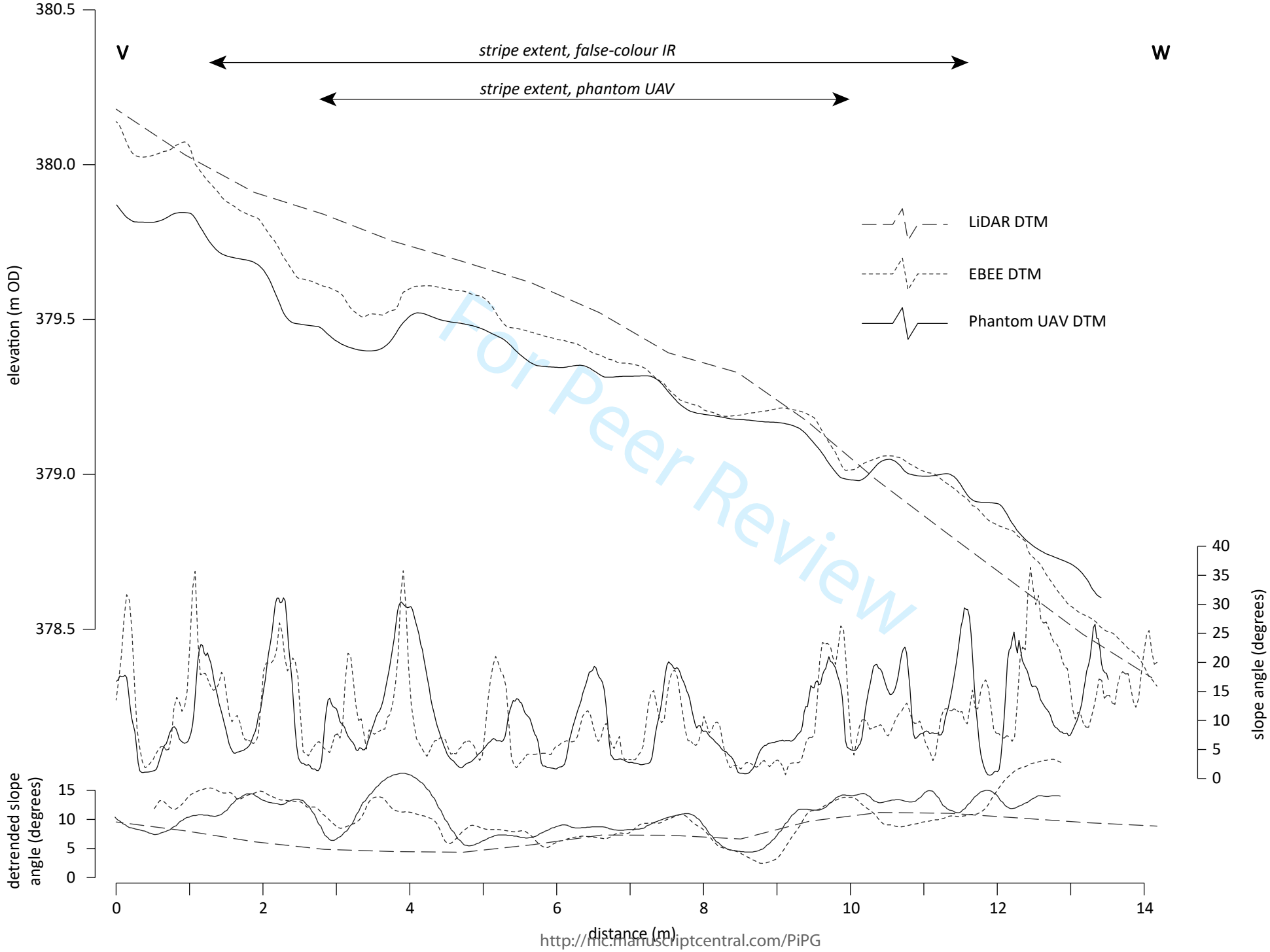

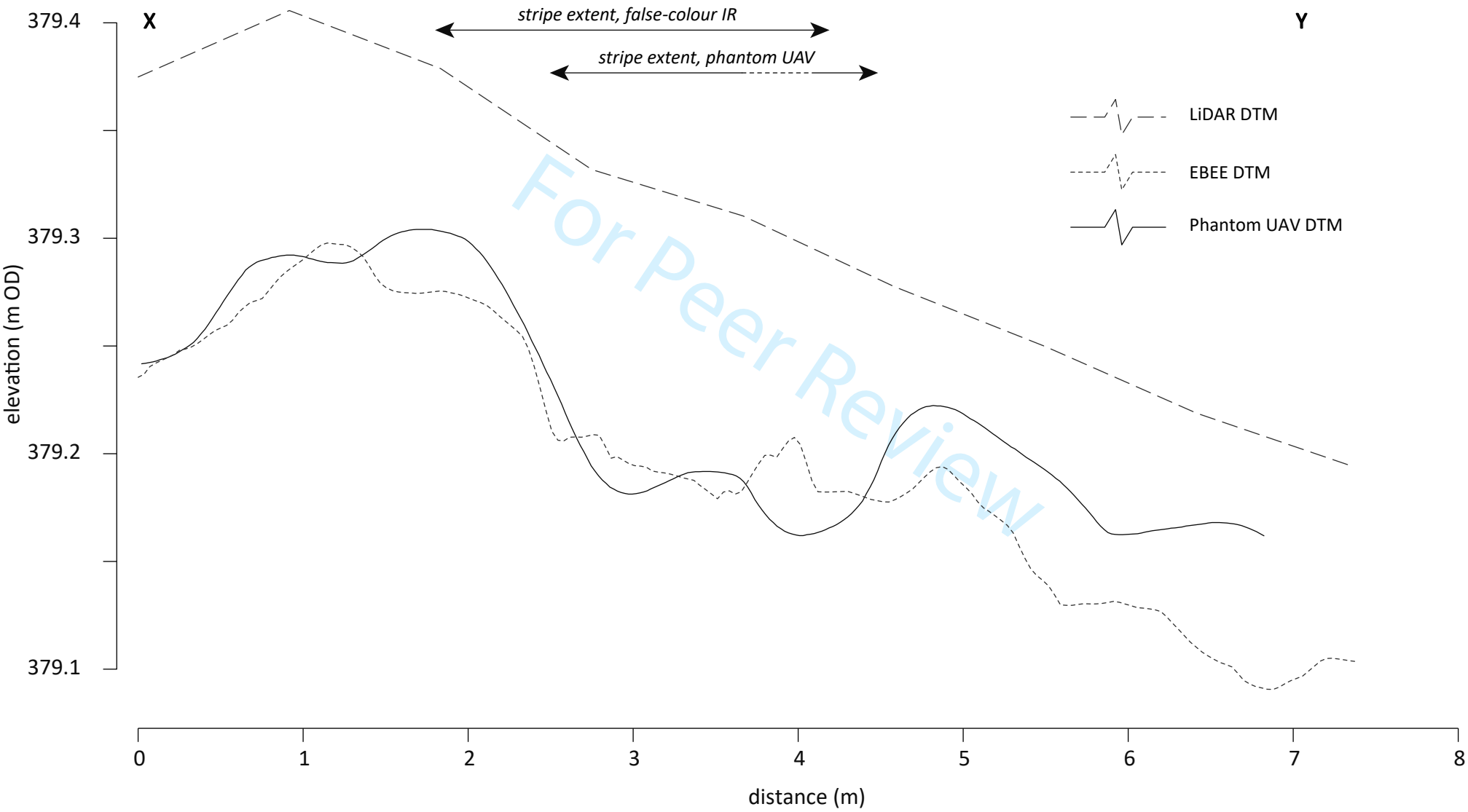

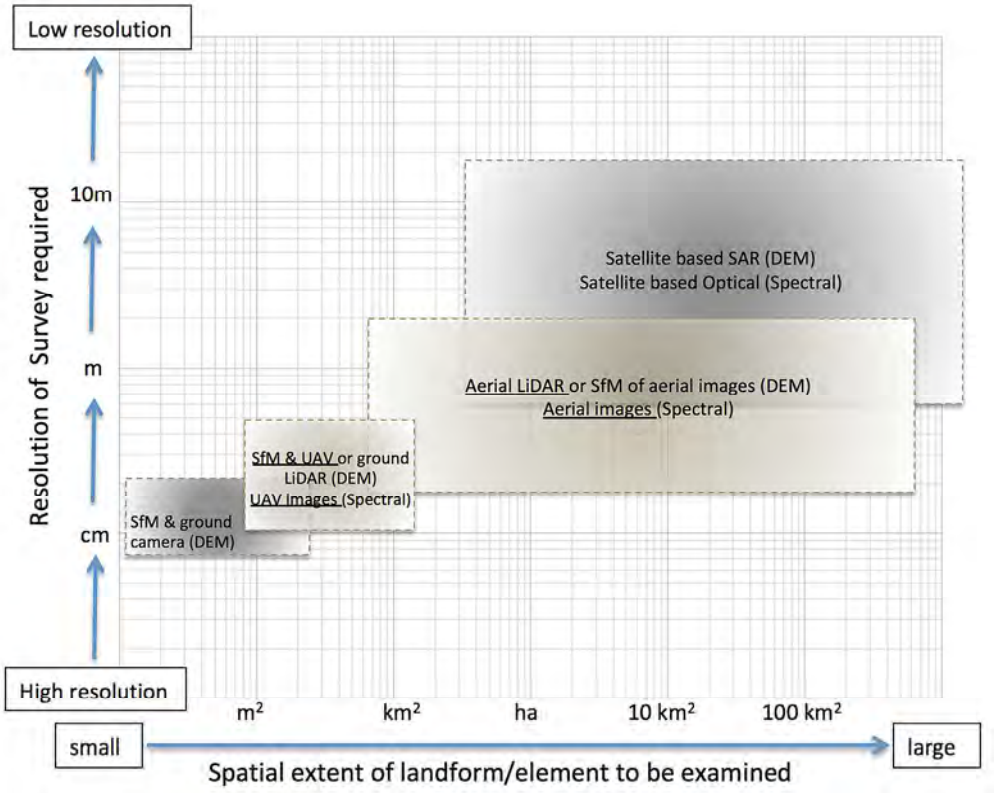

199x161mm (300 x 300 DPI)